IHJPAS. 37 (1) 2024
Ibn Al-Haitham Journal for Pure and Applied Sciences
Journal homepage: jih.uobaghdad.edu.iq
PISSN: 1609-4042, EISSN: 2521-3407

Development of the Properties of Zinc Polycarboxylate Cement Used as a Basis for Dental Fillings Using Zink Oxide Nanoparticles Prepared by Green Chemistry Method

[1]Noor Jabbar Hattab* [2]Entisar Eliwi Laibi [3]Mohammed Mhna Mohammed

[1,2]Department of Chemistry, College of Education for Pure Sciences, Ibn Al-Haitham, University of Baghdad, Baghdad, Iraq.
[3]Center of Excellence Geopolymer & Green Technology (CEGeoGTech), Universiti Malaysia Perlis, 02600, Arau, Perlis, Malaysia

*Corresponding Author: nooralhattab23@gmail.com

Received 7 May 2023, Received 22 June 2023, Accepted 19 June 2023, Published 20 January 2024

doi.org/10.30526/37.1.3470

Abstract

Most dental supplies don't seem to be much of a barrier against germ infiltration. Therefore, the filling must be done with perfect caution and high antimicrobial effectiveness. When dental erosion occurs due to germs that lead to caries, a dental filling is used, creating a small microscopic space between the dental filling and the root end infiltration. This allowed the tooth to be penetrated for the second time, which was the research problem. Adding two compounds to antibacterial fillers (zinc polycarboxylate cement) made them work better: Firstly, was zinc oxide (ZnO) that was made chemically, and secondly, was green ZnO nanoparticles that were made from orange peels and mixed with ZPCC in different amounts. The study was conducted on the formed nanocomposite using FTIR, UV-vis, FESEM, sitting time, and antibacterial measurements. The biological activity was tested using *Staphylococcus aureus*, *Escherichia coli*, and *Candida albicans.*

Keywords: Zinc polycarboxylate cement, Zink oxide nanoparticles, Green chemistry, ZnO-ZPCC, Green-ZnO-ZPCC.

1. Introduction

Dental cements available on the market vary significantly in their chemical consistency. Therefore, there is a significant difference in the mechanical properties in addition to the difference in the physical properties and a substantial difference in the biological properties due to their unique physicochemical properties [1-3].

The ZPCCs are produced by heating zinc oxide (ZnO) and hydropolyacrylic acid. Cement is commonly used for luting permanent restorations due to its strong compatibility with pulp. The

principal pain usually associated with luting was not developed when casting repairs using ZnO polycarboxylate cement ZPCC were introduced. These cement components, however, shrink at a more extensive area than zinc phosphate cement. Since obtaining a reduction in size, this leads to cross-linking of polyacrylic acid chains with zinc atoms [4,5]

Nanotechnology is one of the most important technologies used recently, as it enters many fields and works on it may impact the safety of a bulk repair. Oxide metals Ceramics, catalysis, semiconductors, medicine, space exploration, batteries, capacitors, absorbents, agriculture, defense, textiles, biological and chemical sensors, optoelectronics, and the food industry are just some of the areas where nanobodies have found significant application in recent years [6-12].

Zinc oxide is an inorganic semiconducting substance. Every zinc atom in wurtzite is tetrahedrally coupled with four oxygen atoms, making the material's structure thermodynamically stable at ambient temperatures. Zinc oxide has a large band gap of 3.1–3.3 eV4. It has several potential applications in many fields, including biosensors, cosmetics, medication transporters, and antibacterial agents. Some procedures that can produce ZnO are the microwave method, spray pyrolysis, homogeneous precipitation, mechanical milling, organometallic synthesis, thermal evaporation, and mechanochemical synthesis.

On the other hand, these techniques typically use dangerous reducing agents and organic solvents, the bulk of which are exceedingly reactive and harmful to the environment. Therefore, green synthesis techniques have been employed to create ZnO nanoparticles (ZnONPs) to reduce environmental impact. Green synthesis is a technique for creating NPs with biomedical uses by employing microbes and plants. This approach has various benefits, including affordability, biocompatibility, safety, and environmental friendliness. Furthermore, numerous investigations have demonstrated the potent antibacterial activities of ZnONPs produced using green production techniques [13-16].

Nanoparticles of numerous metals, such as silver, iron, copper, and zinc, have attracted the attention of scientists in recent years [17]. Examples include laser ablation, the sol-gel method, co-precipitation, pyrolysis, microwave irradiation, inert gas condensation, and photoacoustic synthesis. They work on two methods of physical or chemical synthesis, and the most important characteristics of these methods are that they are very dangerous and take a long time. It is also costly to complete. As a result, using green synthesis to produce metallic NPs can solve issues related to conventional techniques. An alternative to traditional methods is the green synthesis of metal NPs using various plant extracts. The ZnONPs have gained significant interest among metal oxide NPs due to their very distinctive chemical properties. ZnONPs have many applications in biotechnology, such as gene transfer, frequently used in nanomedical technologies, drug delivery, biomarkers, nanomedicine, and biosensing. Several researchers have documented the environmentally friendly fabrication of ZnO NPs using different plant extracts, including Calotropis gigantean [18–19], Ocimumbasilicum L.var. Purpurascens [18], Corymbia citriodora [19], Cassia tora L. [20], Sageretiathea [21], Anisochilus carnosus [22], Zingiber officinale [23], Azadirachta indica [24], and Hibiscus rosa-sinensis [25]. One of the most essential advantages of plant extracts used in green chemistry is the absence of compounds that are expected to be toxic, in addition to the presence of natural stabilizers, reducers, and coating agents that make plants and plant parts an ideal platform for nanoparticle synthesis.

2. Materials and Methods

The chemicals and $Zn(NO_3)_2.6H_2O$ used in this investigation were from Sigma Aldrich. Methods for preparing ZnONPs were adapted from those described by Nejati et al. [26].

2.1 Synthesis from renewable sources:-

a. Plant extract preparation

The oranges were cleaned, dried, and peeled wholly to get the extract. The peels are ground into a fine powder after being dried for 12 hours in a food dehydrator. Then, we added 50 milliliters of deionized water to each glass container containing (1 g) of powder and stirred the mixture for three hours. Each mixture was steeped for an hour before being cooked to 60 degrees Celsius in a water bath. After the mixes were filtered, the extracts were stored under argon.

b. ZnO nanoparticle preparation

After heating the extract in a water bath at 60°C for 1 hour, 2 g of $Zn(NO_3)_2.6H_2O$ was added to 42.5 mL of the extract while it was still agitated. The mixes were then dried at 150 degrees Celsius and calcined at 400 degrees Celsius for an hour [28]. A chemical equation showing the reaction of orange peels to produce G-ZnO-NPs

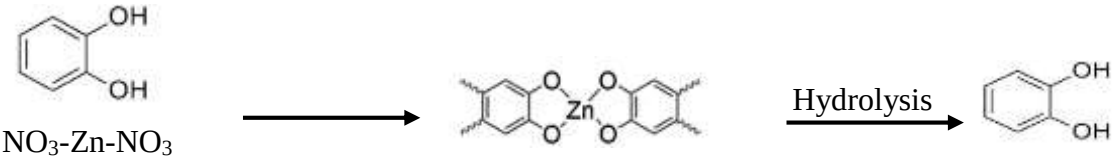

+ NO_3-Zn-NO_3

+ZnO+NO_2+H_2O

2.2 Preparation of composites

The compound was created by mixing 4g of polycarboxylic zinc cement with (0.2 , 0.5 , 1) g of chemical ZnO and green G-ZnO while it was at room temperature. The Impact of Antimicrobials is available in version 2.4. Nanocomposites ZPCC, ZnO-ZPCC, and G-ZnO-ZPCC were tested on three different microbial strains by TM Media Titan Biotch Ltd for their antibacterial activity [29, 30].

3. Results and Discussion

3.1 Characterization

Several methods, such as UV-Vis absorption and FTIR Spectra Analysis, were used to examine powder samples to learn how ZnO NPs affected the physical and chemical properties of ZPCC.

3.2 Ultraviolet-visible spectroscopy (UV-Vis Spectroscopy).

Green chemistry, or using the phytochemicals for nanomaterial creation, is a recent development that has allowed scientists to gain control over the size and shape of Nano materials. Phytochemicals present in a given environment decrease metal ions to Nano metals. Thus, these chemicals function both as reducing agents and as stabilizing agents. Reaction progression can be observed in the visible and ultraviolet spectra. The surface plasmon resonance absorption peak is used to figure out how metal ions are reduced to nanometals. This is where electron vibrations are captured in the conduction band by electromagnetic waves. **Figure 1a** shows a single peak at 256 nm in the orange peel extract. The bioactive substances and stabilizers, flavonoids and tannins, found in eucalyptusm spherical extract [31] make hydroxide groups available for nanomaterial production. Phytochemical materials have the ability to reduce and stabilize metal ions at the nano scale [32], and they can also supply Nano materials in a wide range of dimensionalities thanks to their antioxidant and chemical-free nature. **Figure 1b** displays the UV-Vis spectra of ZPCC, which reveals an absorption maximum at 244 nm. Figure 1c shows the UV-Vis spectra of the produced ZnONPs, which exhibit an absorption maximum (3.872 at 338 nm). It's obvious that it's heading in the direction of the spectral line [33, 34]. In **Figure 1d**, we see the results of UV-Vis absorption tests performed on ZnONPs extracted from Atalantia monophylla, with wavelengths ranging from 300 to 1000 nm. The ZnO has a very strong absorption peak at 372 nm and a broad, selective absorption value. It has been found that ZnONPs have absorption spectra between 330 nm and 370 nm. This research corroborates the aforementioned conclusions [35].

Absorption band shifts were readily apparent after adding the ZnNPs. Nanocomposites of ZnO and zinc phosphoric acid The peak intensity, roughly at 1570 and 1420 cm^{-1}, increased as the amount of nanomaterials increased. The absorption peaks of cement were modified due to interactions with NPs.

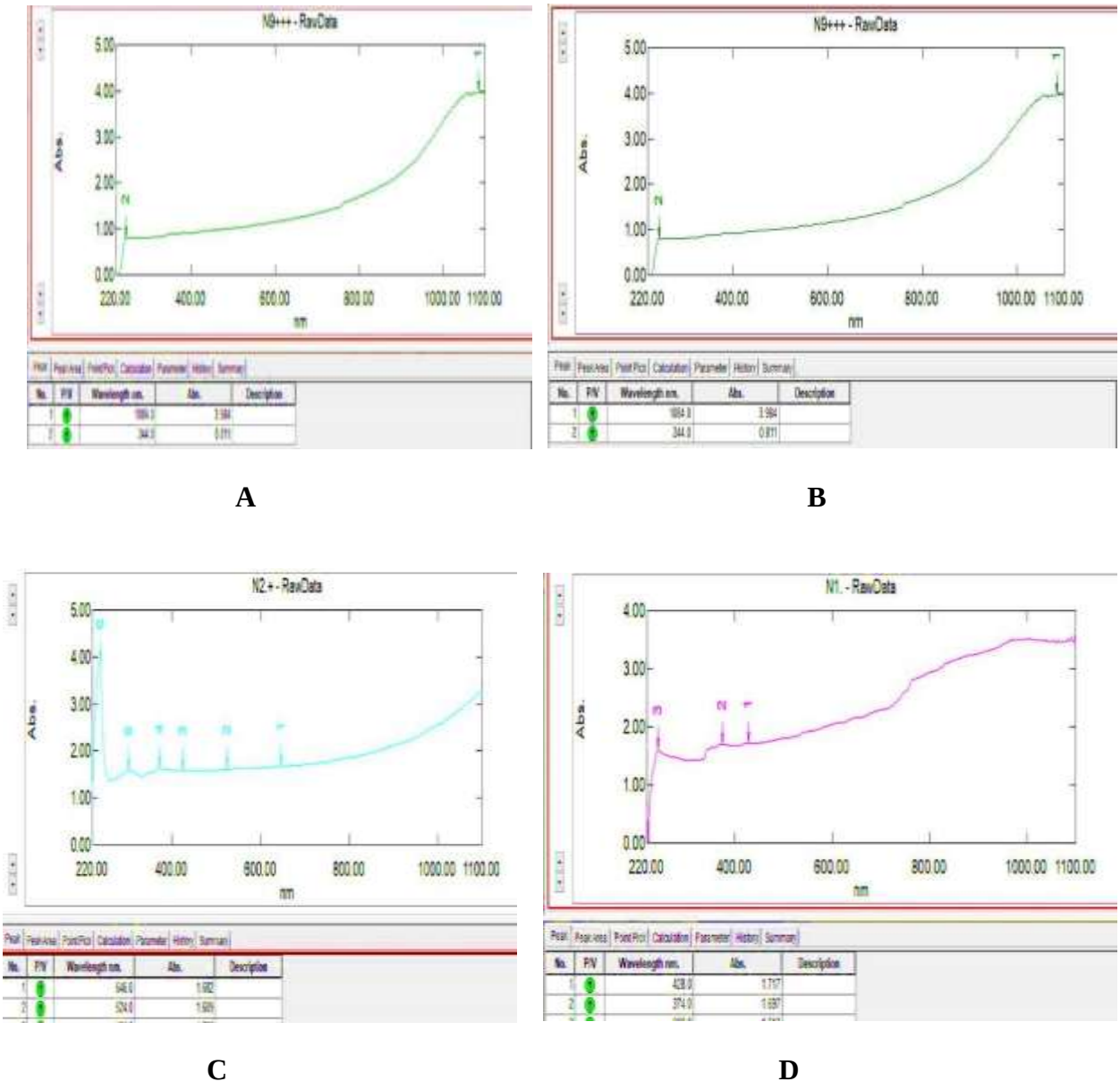

Figure 1. The UV-vis pattern of A) orange peel extract, B) ZPCC, C) ZnNPs, D) green ZnNPs

3.3 Fourier-transform infrared spectroscopy (FTIR)

Orange Peel Extract, ZPCC, ZnNPs, Green ZnNPs, Zn-ZPCC, and G-Zn-ZPCC FTIR Spectra Analysis (SHIMADZU) Recorded Materials. As can be seen, the broad band at approximately 3441.01 cm^{-1} that appears in the spectra of all samples is caused by the gradual absorption of water molecules onto the specimens' surfaces. The FTIR analysis spectrum of zinc polycarboxylate (ZPCC) cement is shown in **Figure 2b**. It exhibits a peak at approximately 1562.34 cm^{-1}, which is related to the stretching of the carboxyl group's absorption of C=O.

The orange peel extract's FTIR spectrum shows two peaks at 1639.49 cm^{-1} and 1415.75 cm^{-1}, respectively, which are caused by the stretching peaks of the C=C and C=O groups.

Peaks at 455.20cm^{-1} were seen in the FTIR spectra of ZnO nanobodies made using a chemical process **Figure 2c** and ZnO NPs made using a green approach **Figure 2d**. The stretching vibration of the Zn-O bonding is related to the peaks in **Figure 2d** at 443.63cm^{-1}, and the FTIR spectra of ZnO NPs produced using the green technique also showed a band at roughly 1485.19 cm^{-1}. Our experiments validated the conclusion that it may be caused by vibrations of a leftover organic chemical in the plant extract in the solution of NPs.

After adding the chemical and green ZnONPs, to zinc polycarboxylate cement (ZPCC), to give ZnO-ZPCC & G-ZnO-ZPCC nanocomposites, **Figures 2e**, 2f, which appear to peak at (429.49) and (416.62), respectively, as well as the peaks of (ZPCC), which point to the fabrication of ZnO-ZPCC and G-ZnO-ZPCC Composites, displayed the FTIR spectra of ZnO-ZPCC and G-ZnO-ZPCC. The two bands at 1643.63 and 1604.cm^{-1} in the FTIR analysis of orange peel extracts are thought to be the bands operating for C=C and C=O, respectively. The stretching of the O-H and N-H groups found in carbohydrates, proteins, and fatty acids is related to the broad peak concentered at 3400 cm^{-1}. The esters groups carbonylic are linked to the signal at 1742 cm^{-1}. The bands at 1098 cm^{-1} and 1023 cm^{-1}, which are the cellulose and hemicellulose bands typical of lignocellulose materials, are related to CO stretching. **Figure 2b** observes the FTIR spectrum of a (ZPCC), which exhibits the essential peak at 1558.48 cm^{-1}, showing taxa with an expansion pattern for the adsorption of the C=O carboxyl group in the cement salt.

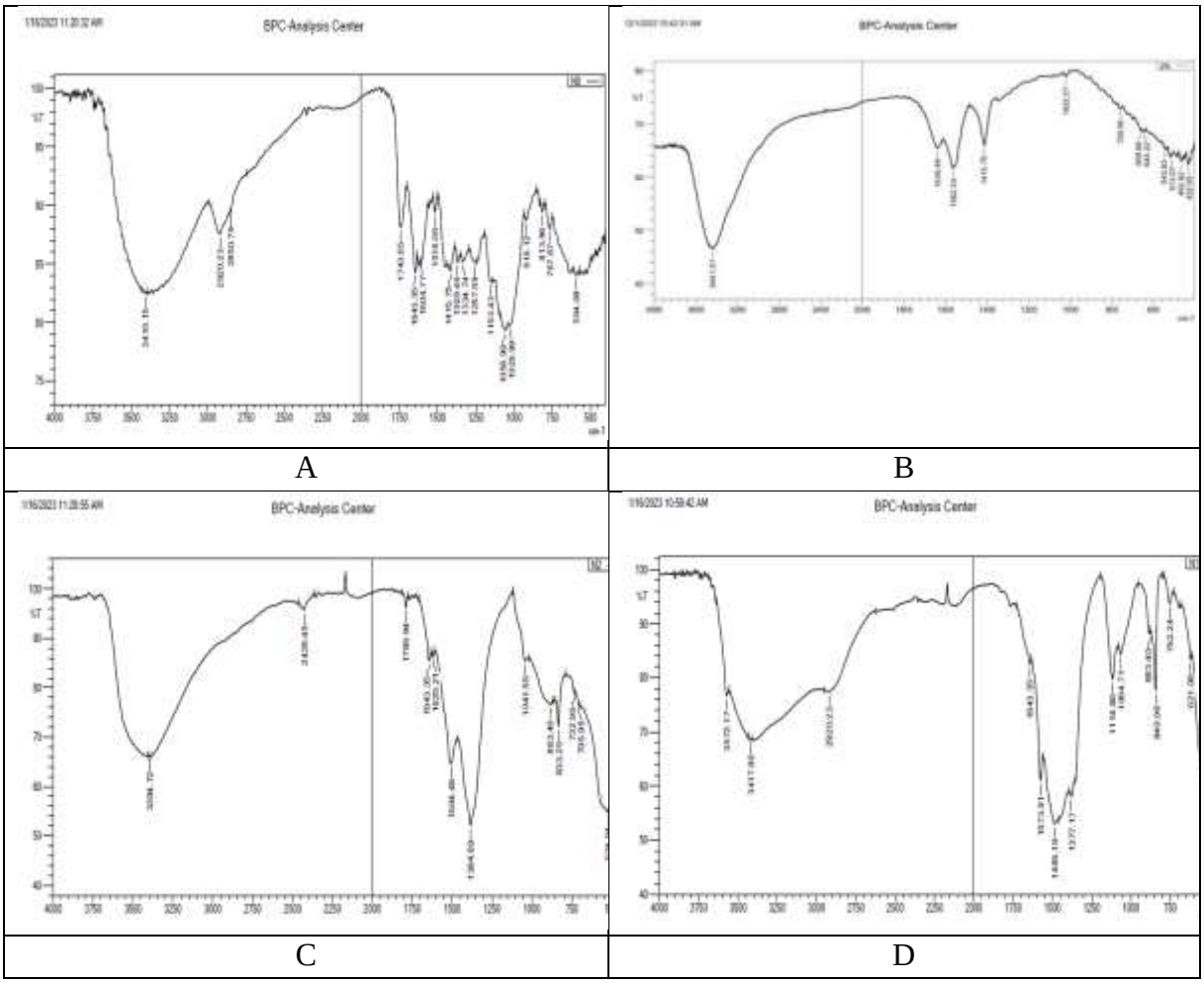

A B

C D

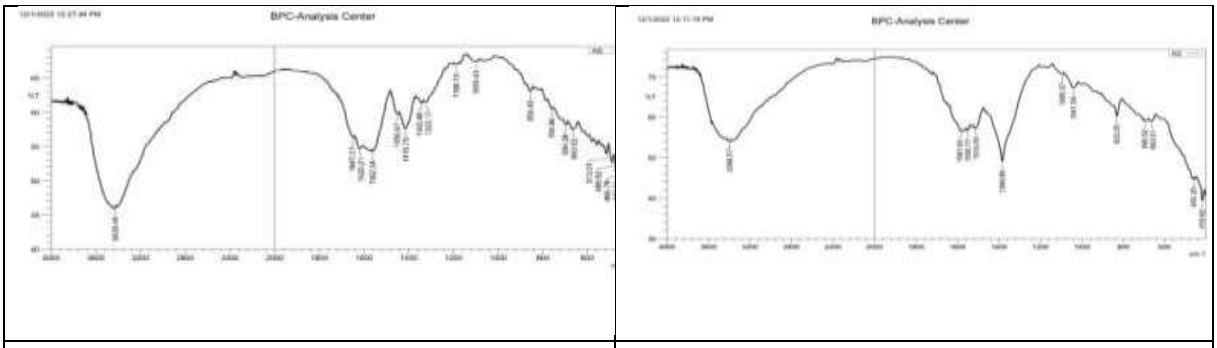

E F

Figure 2. The FTIR spectra analysis of the following materials: a) orange peel extract; b) ZPCC; c) green ZnNPs; d) ZnNPs; e) Zn-ZPCC; and f) green Zn-ZPCC.

3.4 The FESEM and EDS analysis

Measurements with a scanning electron microscope (FESEM) revealed the samples' morphological characteristics and surface features. As shown in **Figure 3**, the Zinc Polycarboxylate cement structure has a flat, homogeneous morphological structure with distinct interstitial porosity channels arranged on a large surface area, and the particle size is around (66 nm). Cement is an excellent carrier because of its high pore surface area and large pore size [37]. **Figure 4** shows FESEM images taken after (0.25 g) of ZnONPs prepared via the chemical method were added to the cement, and a (ZnO-ZPCC) composite was formed. The ZnONPs, which appear as white spherical particles, fill the porous channels between the surfaces of the cement, thereby improving its mechanical properties. Besides the fact that microorganisms have a hard time penetrating ZnO-ZPCC, we can see from the figure that the particles' measured dimensions are roughly 131.3 nm, which means that the dimensions measured were less for the composite (ZnO-ZPCC) than they were for cement alone [38]. The FESEM pictures of the (G-ZnO-ZPCC) composite after adding 0.25 g of ZnONPs synthesized using green chemistry from utilized (orange peel) extract are shown in **Figure 6**. Smaller than expected particle sizes (53.68 nm) and the presence of interstitial porous spaces.

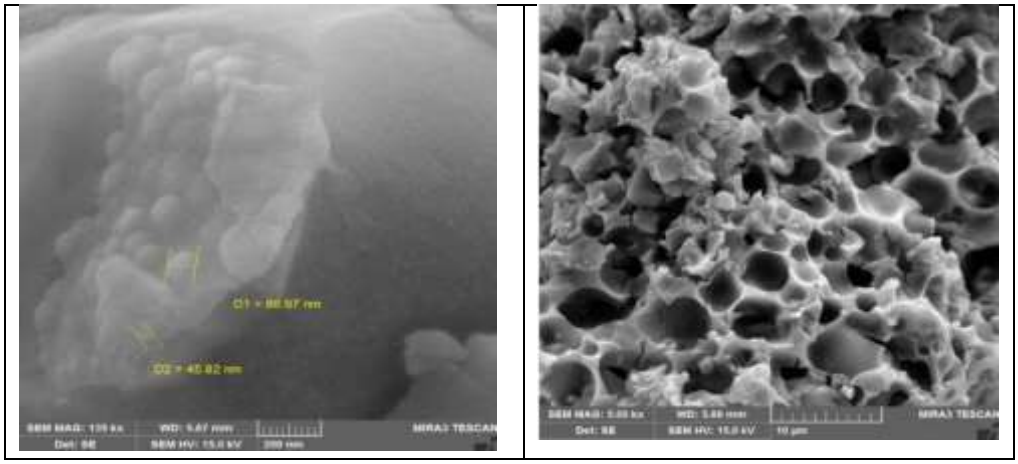

Figure 3. The FESEM analysis For ZPCC

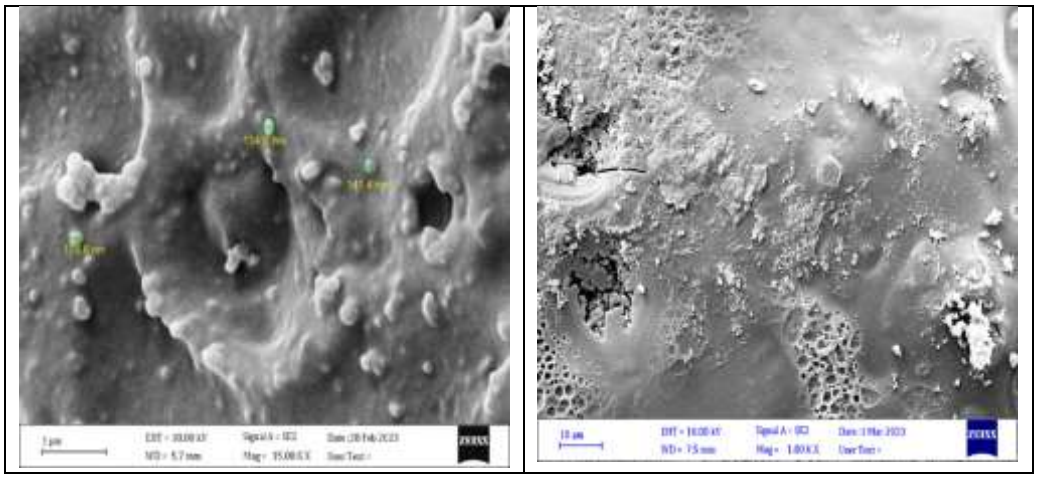

Figure 4. The FESEM analysis For (ZnO-ZPCC)

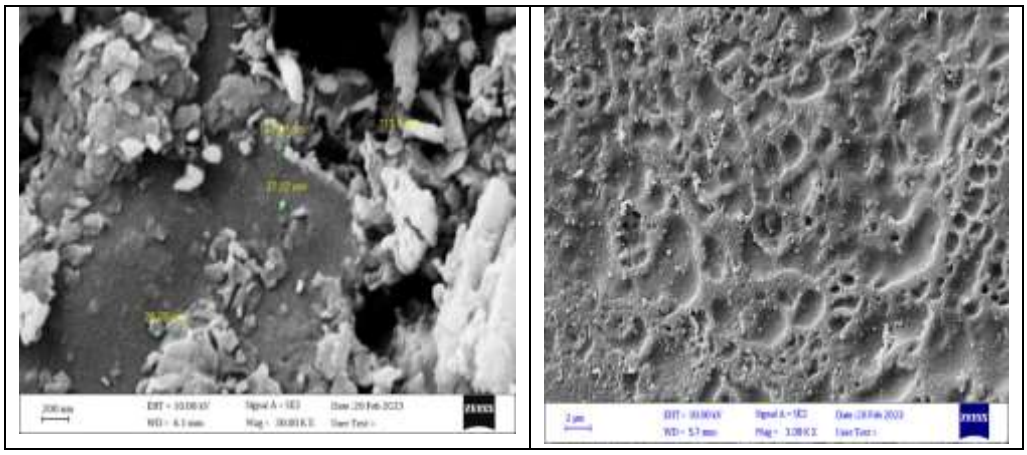

Figure 5. The FESEM Analysis For (G-ZnO-ZPCC)

When it is set, polycarboxylate cement doesn't generate much heat like other types of dental cement. The powder-to-liquid ratio, the presence of additives, the particle size, and the concentration and molecular weight of polyacrylic acid all play a role in the setting time [39,40]. While all other factors were held constant, using ZnNPs as an antibacterial reagent affected the cement setting times. Cement averaged a setting time of 4.5 minutes throughout its many varieties. The optimal inclusion of 0.31 g reduced the setting time to roughly 3.3 minutes by influencing the setting reactions of the produced cement compounds. The setup reaction might be because of the catalytic activity of the ZnONPs, which starts the reaction between ZnO and PAA when the cement mixture is being made. According to this criterion, smaller crystals are more reactive than larger ones since they have a higher surface area. It was also found that adding silver NPs to the cement increased its density. The designer may now breathe a little easier regarding finances [40,41].

3.5 Place and timing

The ZPCC's setting time reaction is determined by the molecular weight and concentration of the polyacrylic acid, the strength of the ZnO, the powder-to-liquid ratio, the presence of additives, and the particle size. Setting rates of the produced cement were influenced while maintaining these parameters and introducing ZnONPs as a microbiological reagent. The entire cement job was finished in 4.3 minutes. Cement composites' setting times are affected by the

amounts of ZnONPs added, with the optimal amount being 0.32 g, resulting in a setting time reduction of roughly 3.5 minutes. ZnONPs catalyze to speed up the cement mixture production reaction between ZnO and PAA, which can be linked to the shorter reaction time observed. Surface area is another indicator of this criterion, with smaller particles being more reactive than larger ones because of their greater surface area. ZnONPs were also shown to increase the volume of the finished cement. This finding provides the designers with an excellent cost-benefit consideration zone [42].

3.6 Antibacterial effects

Since agar diffusion is the standard method for measuring the efficacy of antimicrobials, it was employed in this study. The infected culture environment must be maintained at room temperature for two hours before the breeding phase, which is a significant step in this method [40]. Not being able to tell the difference between bactericidal and bacteriostatic impacts is one of the many drawbacks of this approach [41,42]. To a greater extent than the inhibitory impacts of a drug alone, the infusibility of the objective through surroundings determines the efficacy

and areas of inhibition [43]. There may also be interference from factors such as the length of incubation, the number of inoculated cells, and the extent to which the inoculated cells come into contact with the agar [44]. Materials' antimicrobial impacts can be compared under similar experimental conditions [45, 46] if almost all relevant factors are appropriately managed, allowing for proportional and reproducible results. Our research focused on a specific group of bacteria that were either causal agents of genuine endodontic illnesses or were somehow associated with instances that proved difficult to treat [47].

Even though facultative and aerobic microorganisms are always present in essential contagions [46], they have been found more often in treatment states that last a long time, in flare-ups, and in states that don't work. Microorganisms such as *E-coil*, *Staphylococcus aureus*, and *Candida albicans* can cause severe infections in the root canal [48]. According to the study's findings in **Table 1** and **Figure 6**, the antibacterial effects of ZPCC were enhanced by adding NPs in different concentrations when confronting bacterial cells, including *Escherichia coli, Staphylococcus aureus,* and *Candida albicans*. However, *S. aureus's* resistance to antibiotics was consistent. Antimicrobial efficacy was significantly increased against *Escherichia coli* and *Staphylococcus aureus,* but against *Candida albicans*, it was reduced considerably.

The ZPCC's antimicrobial effectiveness appears to be linked with increased pH values. ZPCC has a pH of around 10, rising to about 12.0 when adding NPs. It is generally accepted that pH levels above 12 effectively inhibit the growth of virtually all microorganisms. The ZPCC's antifungal properties may be attributed to its higher pH or the chemicals it secretes. Due to their small size, NPs may be more effective than ions at inhibiting microbial growth at equivalent doses. There was also a correlation between particle size and antibacterial efficacy [49].

It was shown that smaller particles had a more excellent bactericidal action than larger ones. In **Figure 6**, a comparison of the antimicrobial efficacy of ZPCC and ZnO-ZPCC nanocomposites in terms of increasing the inhibitors, and in Figure 8, a similar comparison was seen for ZPCC and G-ZnO-ZPCC composites [50-52].

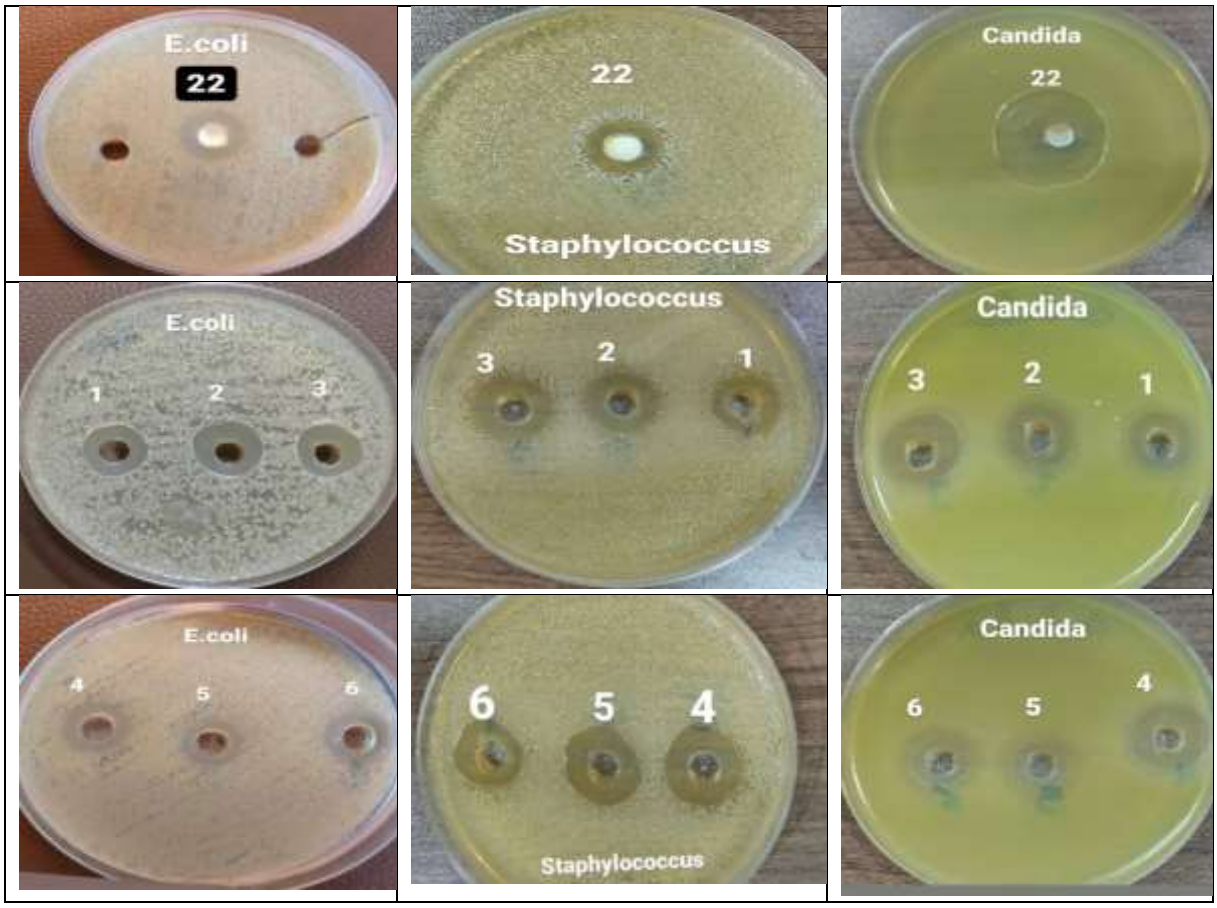

Figure 6. Green ZnONPs-ZPCC composites, zinc polycarboxylate cement (ZPCC), and ZnONPs-ZPCC exhibit antimicrobial activity as measured by a fold increase in the diameter zone

3.7 Analysis by Statistics

For the statistical evaluation of the gathered data, SPSS version 17 (Chicago, USA) was employed. Levene and Shapiro-Wilk tests were used to determine homogeneity and normality, respectively. A mean SD format was used to present the data.

Figure 7 and **Table 1** depict the means and standard deviations of the growth inhibition diameters for each of the microorganisms studied. The independent t-test determines whether there are statistically significant differences between groups on three scales (0.2, 0.5, and 1g). Statistical research demonstrated that at 0.2, 0.5, and 1 gm for Candida and 1 gm for Escherichia coli, there were statistically significant differences between NPs and ZPCC. It also indicated a standard range of growth inhibition diameters for the ZPCC, ZnO-ZPCC, and G-ZnO-ZPCC groups against the bacteria examined [51].

Table 1. displays the mean and standard deviation of the growth inhibition diameters of the previously tested microorganisms per mm of ZPCC and ZnO-ZPCC composite

	Weight of ZnO- ZPCC								
Bacterial	0.2g			0.5g			1g		
	E.coli	Staph	Candiad	E.coli	Staph	Candiad	E.coli	Staph	Candiad
ZnO-NPs	15.333	15.333	14.000	15.667	16.000	15.667	21.333	18.300	18.333
ZPCC	13.000	18.333	30.000	13.000	18.333	30.000	13.000	18.333	30.000
p-value	0.07999	0.03994*	0.00009**	0.05598	0.07999	0.00014**	0.00113**	0.97526	0.00031**

* The difference is considered statistically significant (under 0.05).

** The difference is considered highly statistically significant (under 0.01).

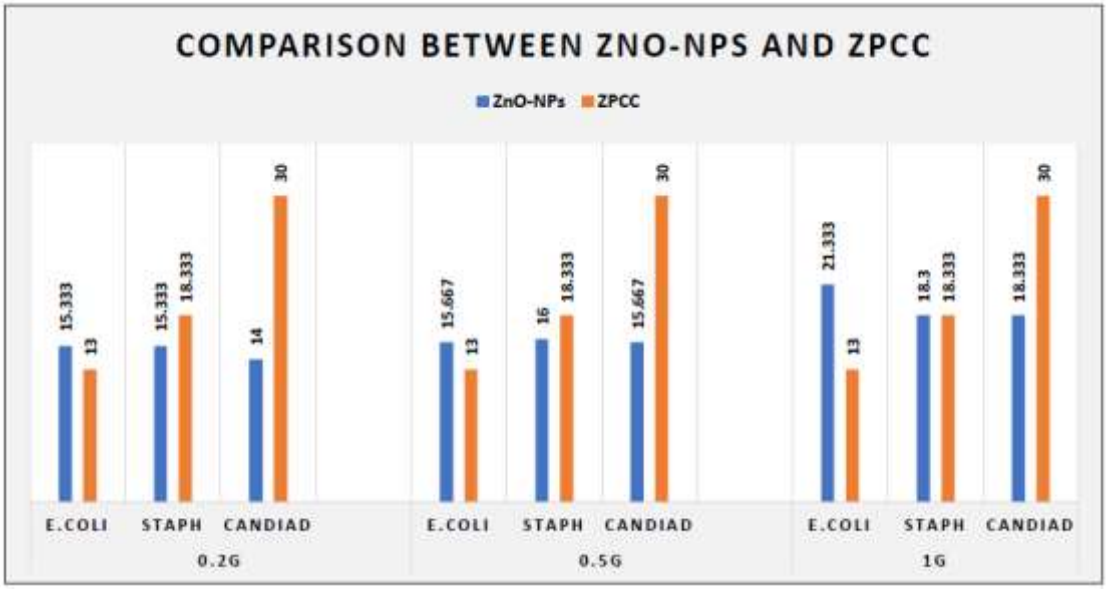

Figure 7. Comparison of the mean values of the studied microorganisms per millimetre in the ZPCC and ZnO-ZPCC composite

Table 2 and **Figure 8** show the typical and standard deviations of the sizes at which the development of the several microorganisms examined was inhibited. The same three measures (0.2, 0.5, and 1) g are used to assess whether or not there are statistically significant differences between groups using independent t-tests. Demonstrated the findings of the statistical analysis of the normal distribution of growth inhibition diameters in the ZPCC and ZnO-ZPCC groups against the tested microorganisms and showed statistically significant differences between G-ZnO-NPs and ZPCC at (0.2, 0.5, and 1) g for *Escherichia coli*, and additionally 1.0 g for staphylococci.

Table 2. Growth inhibition diameters of the tested microorganisms per mm of ZPCC and G-ZnO-ZPCC composite were compared to find the mean and standard deviation.

	Weight of G-ZnO-ZPCC								
Bacterial	0.2g			0.5g			1g		
	E.coli	Staph	Candiad	E.coli	Staph	Candiad	E.coli	Staph	Candiad
G-ZnO-NPs	15.667	16.000	17.333	17.000	13.000	10.000	13.667	15.333	12.667
ZPCC	13.000	18.333	30.000	13.000	18.333	30.000	13.000	18.333	30.000
p-value	0.05598	0.07999	0.00022**	0.01613*	0.00595**	0.00004**	0.54128	0.03994*	0.00007**

* The difference is considered to be statistically significant under 0.05.
** The difference is considered to be highly statistically significant under 0.01.

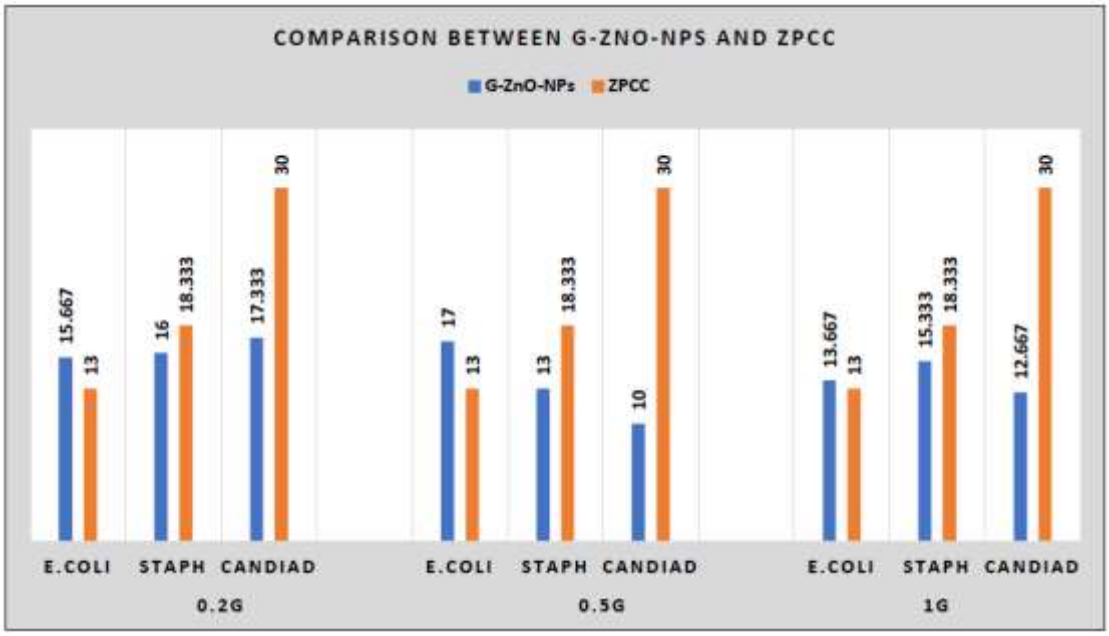

Figure 8. Comparison of the values between the medium diameters for growth inhibition vs. (microorganisms) previously examined per mm of ZPCC & G-ZnO-ZPCC compound.

4. Conclusion

The agar diffusion assays reveal that adding different amounts of ZnONPs to ZPCC using chemical and environmentally friendly methods results in ZnO-ZPCC and G-ZnO-ZPCC composites, both of which exhibit enhanced antimicrobial activity against a clinical isolate of three important microorganisms used in this study*: E-coil, S. aureus*, and *C. albicans*. ZnO-ZPCC and G-ZnO-ZPCC composites have quicker setting times than the original ZPCC and are produced when ZnONPs are added to the ZPCC mixture. The amount of chemical and green ZnONPs supplied affects how quickly the cement composites set; the ideal addition is 0.2 g, which brings the setting time down to about 3.5 minutes. The reduced reaction time observed can be attributed to ZnONPs acting as catalysts to accelerate the cement mixture manufacturing reaction between ZnO and ZPCC. Another indicator of this criterion is surface area, with

smaller particles having more reactivity than bigger ones due to their larger surface areas. It was also demonstrated that ZnONPs increased the amount of the finished cement. Thanks to this discovery, the designers now have a helpful area for cost evaluation. It is conceivable to link ZPCC to it further.

Acknowledgment

The authors thank the staff at the Department of Chemistry/ College of Education for Pure Sciences at (Ibn Al- Haitham)/ University of Baghdad for their assistance in performing this research.

Conflict of Interest

The authors declare that they do not have any competing interests.

Funding

There is no financial support.

Ethical Clearance

This work has been approved by the Scientific Committee at the University of Baghdad/ College of Education for Pure Sciences (Ibn Al-Haitham).

References

1. Milutinović-Nikolić, A.D.; Medic, V.B.; Vuković, Z.M. Porosity of different dental luting cements. *Dental Materials*, **2007**, 23(*6*), 674–678. https://doi:10.1016/j.dental.2006.06.006.
2. Sachdeva, H.; Sharma,N.; Sharma, A.; Shrivastava, R. Plant-extract mediated synthesis of copper – and iron- based nanoparticles for various applications. *NanoWorld J.*, **2022**, *8*(S1), S162-S167. https://doi: 10.17756/nwj.2022-s1-026.
3. Mohammed, A.; Sulaiman, A.F. and Al-Abodi, E.E. A Review: Antibiological effect of modified silver nanoparticles using plants extract. *Annals of the Romanian Society for Cell Biology*,**2021**, *25*(*6*),13428-13432. http://www.annalsofrscb.ro/index.php/journal/article/view/8135.
4. Hadi, K.; Al- Saadi, T.M. Investigating the structural and magnetic properties of nickel oxide nanoparticles prepared by precipitation method. *Ibn AL-Haitham Journal For Pure and Applied Sciences*, **2022**, *35*(*4*), 94–103. https://doi.org/10.30526/35.4.2872.
5. Emad, A. Development of dental fillings in terms of properties using silver nanoparticles and plant extracts. M.Sc. Thesis, The college of College of *Education Ibn Al-Haytham for Pure Sciences–University , Iraq*, **2021**, *16*, 943–946.
6. Hussein, A.; Al-Abodi, E.E. A review article: Green synthesis by using different plants to preparation oxide nanoparticles. *Ibn AL-Haitham Journal For Pure and Applied Sciences*, **2023**, *36*(*1*), 246–259. https://doi.org/10.30526/36.1.2933.
7. Gebre, S. H.; Sendeku, M. G. New frontiers in the biosynthesis of metal oxide nanoparticles and their environmental applications: An overview. *SN Applied Sciences*, **2019**, *1*(*928*). https://doi.org/10.1007/s42452-019-0931-4.
8. AL-Abodi, E.E.; Farouk, A. preparation characterization and electrical study of new polymeric mixture (Consist of Three Polymers) nanocomposites. *Journal of Physics: Conference Series*, **2018**, 1003(1), 012014.

https://ui.adsabs.harvard.edu/link_gateway/2018JPhCS1003a2014A/doi:10.1088/1742-6596/1003/ 1/012014.

9. Hadi, K.; Al- Saadi, T.M. Investigating the structural and magnetic properties of nickel oxide nanoparticles prepared by precipitation method. *Ibn AL-Haitham Journal For Pure and Applied Sciences*, **2022**, *35*(*4*), 94–103. https://doi.org/10.30526/35.4.2872.
10. AL-Rubaye, H. I.; AL-Rubaye, B. k.; Al-Abodi, E. E.; Yousif, E. I. Green chemistry synthesis of modified silver nanoparticles. *Journal of Physics: Conference Series*, **2020**, *1664*(*1*), 012080. http://dx.doi.org/10.1088/1742-6596/1664/1/012080.
11. Al-Abodi, E.E; Al-Saadi, T.M.; Sulaiman, A.F.; Al-Khilfhawi, I.J. Biosynthesis of silver nanoparticles by using garlic plant Iraqi extract and study antibacterial activity",*3rd Woman Scientific Conference of woman science collage-Baghdad University*, **2016**.
12. Kadhim, R. M.; Al-Abodi, E. E.; Al-Alawy, A.F. Citrate-coated magnetite nanoparticles as osmotic agent in a forward osmosis process. *Desalination and Water Treatment*, **2018**, *115*, 45–52. http://dx.doi.org/10.5004/dwt.2018.22456.
13. Sabbar, H.A. Adsorption of phenol from aqueous solution using paper waste. *Iraqi Journal of Chemical and Petroleum Engineering* **2019**, *20*(1), 23–29. https://doi.org/10.31699/IJCPE.2019.1.4.
14. Almuslamawy, H.A.; Hashim, R.A.; Aldhrub, A.H.; Mouhamad, R.S. Biosorption of pollutants in Diyala river by using Irrigated vegetables. Asian *Journal of Water, Environment and Pollution*,**2023**, *20*(*2*),51-57. https://doi:10.3233/AJW230024.
15. Sulaiman, A.F.; Alwan, W.M.; Salman, S.A.; Al-Abodi, E.E.. A Comparative study of chemical compounds and anti-bacterial efficacy of different Allium Cepa plant extracts. *Syst. Rev. Pharm.*, **2021**,*12*(*1*),45-48.https://www.sysrevpharm.org/articles/a-comparative-study-of-chemical-compounds-and-antibacterial-efficacy-of-different-allium-cepa-plant-extracts.pdf.
16. Latif, I.; AL-Abodi, E.E.; Badri, H.D.; Al Khafagi, J. Preparation, characterization and electrical study of (carboxymethylated Polyvinyl Alcohol/ZnO) nanocomposites. *American Journal of Polymer Science*, **2013**, *2*(*6*), 135–140. https://doi: 10.5923/j.ajps.20120206.01.
17. Sadiq, Y. M.; Al-Abodi, E. E. Preparation and characterization of a new nano mixture, and its application as photocatalysis in self-assembly method for water treatment. AIP Conference Proceedings**, 2019,** *2190*(*1*), 020042. https://ui.adsabs.harvard.edu/link_gateway/2019AIPC.2190b0042S/doi:10.1063/1.5138528.
18. Wang, N.; Fuh, J. Y.; Dheen, S. T.; Senthil Kumar, A. Synthesis methods of functionalized nanoparticles: A Review. *Bio-Design and Manufacturing* **2021**, *4*, 379–404. http://dx.doi.org/10.1007/s42242-020-00106-3.
19. Kolahalam, L. A.; Kasi Viswanath, I. V.; Diwakar, B. S.; Govindh, B.; Reddy, V.; Murthy, Y. L. N. Review on nanomaterials: Synthesis and applications. *Materials Today: Proceedings* **2019**, *18(4)*, 2182–2190. http://dx.doi.org/10.1016/j.matpr.2019.07.371.
20. Chaudhuri, S. K.; Malodia, L. Biosynthesis of zinc oxide nanoparticles using leaf extract of Calotropis Gigantea: Characterization and its evaluation on tree seedling growth in nursery stage. *Applied Nanoscience*, **2017**, *7*, 501–512. https://doi.org/10.1007/s13204-017-0586-7.
21. Fan, L.; Tan, B.; Li, Y.; Zhao, Q.; Yuan, H.; Liu, Y.; Wang, D.; Zhang, Z. Upregulation of mir-185 promotes apoptosis of the human gastric cancer cell line MGC803. *Molecular Medicine Reports*, **2018**, *17*(*2*),3115-3122. https://doi: 10.3892/mmr.2017.8206.

22. Zheng, Y.; Fu, L.; Han, F.; Wang, A.; Cai, W.; Yu, J.; Yang, J.; Peng, F. Green biosynthesis and characterization of zinc oxide nanoparticles using*corymbia citriodora*leaf extract and their photocatalytic activity. *Green Chemistry Letters and Reviews* **2015**, *8*(*2*), 59–63. https://doi.org/10.1080/17518253.2015.1075069.
23. Manokari, M.; Shekhawat, M.S. Green synthesis of zinc oxide nanoparticles using whole plant extracts of Cassia tora L. and their characterization. J. Sci. Achiev. **2017**, *2*(*8*), 10–16. https://jsciachv.sinaweb.net/article_80715.html.
24. Abdlzhra, A. F.; Abdllatief, I. A.; Alabodi, E.E.L. Preparation and characterization of silver nanoparticles and study their effect on the Electrical Conductivity of the Polymer Blend (Poly vinyle acitet. Pectin, poly Aniline*). Ibn AL-Haitham Journal For Pure and Applied Science*, **2016**, *29*(*3*), 379–389. https://jih.uobaghdad.edu.iq/index.php/j/article/view/736.
25. Anbuvannan, M.; Ramesh, M.; Viruthagiri, G.; Shanmugam, N.; Kannadasan, N. Anisochilus carnosus leaf extract mediated synthesis of zinc oxide nanoparticles for antibacterial and photocatalytic activities. *Materials Science in Semiconductor Processing* **2015**, *39*, 621–628. http://dx.doi.org/10.1016/j.mssp.2015.06.005.
26. Raj, L.F.A.; Jayalakshmy, E. Biosynthesis and characterization of zinc oxide nanoparticles using root extract of Zingiber officinale. *Oriental Journal of Chemistry* 2015, *31*(1), 51–56. http://dx.doi.org/10.13005/ojc/310105.
27. Bhuyan, T.; Mishra, K.; Khanuja, M.; Prasad, R.; Varma, A. Biosynthesis of zinc oxide nanoparticles from Azadirachta indica for antibacterial and photocatalytic applications. *Materials Science in Semiconductor Processing*, **2015**, *32*, 55–61. http://dx.doi.org/10.1016%2Fj.mssp.2014.12.053.
28. Bala, N.; Saha, S.; Chakraborty, M.; Maiti, M.; Das, S.; Basu, R.; Nandy, P. Green synthesis of zinc oxide nanoparticles using Hibiscus subdariffa leaf extract: Effect of temperature on synthesis, anti-bacterial activity and anti-diabetic activity. *RSC Advances* **2015**, *5*, 4993–5003. https://doi.org/10.1039/C4RA12784F.
29. Abdlzhra, A.F., Abdllatief, I.A., ; Alabodi, E.E.L. Preparation and characterization of silver nanoparticles and study their effect on the electrical conductivity of the polymer blend (Poly vinyle acitet. Pectin, poly Aniline). *Ibn AL-Haitham Journal For Pure and Applied Science*, **2016**,*29*(3), 379–389. https://jih.uobaghdad.edu.iq/index.php/j/article/view/736.
30. Thi, T.U.D; Nguyen, T.T.; Thi, Y. D.; Ta Thi, K. H.; Phan, B. T.; Pham, K. N. Green synthesis of ZnO nanoparticles using orange fruit peel extract for antibacterial activities. *RSC Advances* **2020**, *10*, 23899–23907. https://doi.org/10.1039/D0RA04926C.
31. Emad, A.; Abodi, E.E. Anti-inflammation effects of silver nanoparticles-zinc polycarboxylate cement (AGNPS-ZPCCEM). *Pakistan Journal of Medical and Health Sciences*, **2022**, *16*(*4*), 943–946. https://doi.org/10.53350/pjmhs22164943.
32. Karakece, E. Culture media for detection of Acinetobacter baumannii selective media for detection of a Baumannii. *Journal of Microbiology & Experimentation* **2015**, *2*(*3*),87-90. https://doi.org/10.15406/jmen.2015.02.00046.
33. Mohammed, A.; Sulaiman, A.F.; Al-Abodi, E.E. A Review: Antibiological effect of modified silver nanoparticles using plants extract. *Annals of the Romanian Society for Cell Biology*, **2021** ,*25*, 13428-13432. https://annalsofrscb.ro/index.php/journal/issue/view/30.
34. Mohamed, F.; Sharmoukh, W.; Youssef, A. M.; Hameed, T. A. Structural, morphological, optical, and dielectric properties of pva-pvp filled with zinc oxide aluminum-graphene oxide composite for promising applications. *Polymers for Advanced Technologies*, **2021**, *33*(*3*),1009–1020. https://doi.org/10.1002/pat.5575.

35. Yaghobian, M., & Whittleston, G.A. Critical review of carbon nanomaterials applied in cementitious composites–a focus on mechanical properties and dispersion techniques. *Alexandria Engineering Journal*, **2022**, *61*, 3417-3433. https://doi.org/10.1016/j.aej.2021.08.053.
36. J F Siqueira Jr, J.F.; Favieri, A.; Gahyva, S.M.; Moraes, S.R.; Lima, K.C.; Lopes, H.P. Antimicrobial activity and flow rate of newer and established root canal sealers. *Journal of Endodontics*, **2000**, *26*(*5*), 274–277. https://doi.org/10.1097/00004770-200005000-00005.
37. Sampath, S.; Sunderam, V.; Madhavan, Y.; Hariharan, N. M.; Mohammed, S. S.; Muthupandian, S.; Lawrance, A. V. Facile green synthesis of zinc oxide nanoparticles using Artocarpus hirsutus seed extract: Spectral characterization and in vitro evaluation of their potential antibacterial-anticancer activity. *Biomass Conversion and Biorefinery*, **2023**. http://dx.doi.org/10.1007/s13399-023-04127-7.
38. Fakhari, S.; Jamzad, M.; Kabiri Fard, H. Green synthesis of zinc oxide nanoparticles: A comparison. *Green Chemistry Letters and Reviews*, **2019**, *12*(*1*), 19–24. https://doi.org/10.1080/17518253.2018.1547925.
39. Gao, Y.; Xu, D.; Ren, D.; Zeng, K.; Wu, X. Green synthesis of zinc oxide nanoparticles using citrus sinensis peel extract and application to Strawberry Preservation: A comparison study. *LWT*., **2020**, *126*(1), 109297. http://dx.doi.org/10.1016/j.lwt.2020.109297.
40. Goyal, S. Green synthesis of zinc oxide nanoparticles from plant extract: A review. *International Journal of Green and Herbal Chemistry* **2019**, *8*(*2*),650-659. https://doi: 10.24214/IJGHC/GC/8/3 / 6559.
41. Fraga, R. C.; Siqueira, J. F.; de Uzeda, M. In vitro evaluation of antibacterial effects of photo-cured glass ionomer liners and dentin bonding agents during setting. *The Journal of Prosthetic Dentistry*, **1996**, *76*(5), 483–486. https://doi: 10.1016/s0022-3913(96)90005-0.
42. Klink, M.J.; Laloo, N.; Leudjo Taka, A.; Pakade, V.E.; Monapathi, M.E.; Modise, J. S. Synthesis, characterization and antimicrobial activity of zinc oxide nanoparticles against selected waterborne bacterial and yeast pathogens. *Molecules*, **2022**, *27*(*11*), 3532. https://doi.org/10.3390/molecules27113532.
43. Husain, W. M.; Araak, J. K.; Ibrahim, O. M. S. Green synthesis of zinc oxide nanoparticles from (Punica Granatum L) pomegranate aqueous Peel Extract. *The Iraqi Journal of Veterinary Medicine*, **2019**, *43*(*2*), 6–14. https://doi.org/10.30539/iraqijvm.v43i2.524.
44. Ibraheem, S.; Kadhim, A. A.; Kadhim, K. A.; Kadhim, I. A.; Jabir, M. Zinc oxide nanoparticles as diagnostic tool for cancer cells. *International Journal of Biomaterials*, **2022**, 1–10. https://doi: 10.1155/2022/2807644.
45. Mehata, M. S. Green route synthesis of silver nanoparticles using plants/ginger extracts with enhanced surface plasmon resonance and degradation of textile dye. *Materials Science and Engineering: B*, **2021**, *273*, 115418. https://doi.org/10.1016/j.mseb.2021.115418.
46. Golbarg, H.; Mehdipour Moghaddam, M. J. Antibacterial potency of medicinal plants including artemisia annua and oxalis corniculata against multi-drug resistance E. Coil. *BioMed Research International*, **2021**,*1*, 1–17. https://doi.org/10.1155/2021/9981915.
47. Ravoor, J.; Amirthalingam, S.; Mohan, T.; Rangasamy, J. Antibacterial, anti-biofilm and angiogenic calcium sulfate-nano MGO composite bone void fillers for inhibiting Staphylococcus aureus infections. *Colloid and Interface Science Communications*, **2020**, *39*, 100332. http://dx.doi.org/10.1016/j.colcom.2020.100332.

48. Bouchelaghem, S. Propolis characterization and antimicrobial activities against Staphylococcus aureus and candida albicans: A Review. *Saudi Journal of Biological Sciences*, **2022**, *29*(*4*), 1936–1946. https://doi.org/10.1016%2Fj.sjbs.2021.11.063.
49. Siren, E.K.; Haapasalo, M.P.; Ranta, K.; Salmi, P.; Kerosuo, E.N. Microbiological findings and clinical treatment procedures in endodontic cases selected for microbiological investigation. *International Endodontic Journal*, **1997**, *30*(*2*), 91–95. PMID: 10332242.
50. Molander, A.; Reit, C.; Dahlén, G.; Kvist, T. Microbiological status of root-filled teeth with apical periodontitis. *International Endodontic Journal*, **1998**, *31*(*1*), 1–7. PMID: 9823122.
51. Salman, R. A. Histopathological Effect of Zinc Oxide Nanoparticles on Kkidney and Liver Tissues in Albino Male Mice. *Ibn AL-Haitham Journal For Pure and Applied Science*, **2018**,*31(1)*, 9-14. https://doi.org/10.30526/31.1.1844.
52. Hashim, A.; Al-Abodi, E. E. Photodegradation of Lauth's violet dye using Go-FE3O4-tio2 nanocomposite under Solar Light. *Journal of Physics: Conference Series*, **2021**, *1853*, 012013. https://doi: 10.1088/1742-6596/1853/1/012013.
53. Katafa, A. J.; Hamid, M. K. Influence of zno nanoparticles on Candida Albicans of human male pleural fluid. *Iraqi Journal of Science*, **2020**, *61*(*3*),540–549. https://doi.org/10.24996/ijs.2020.61.3.10.
54. Imran, H. J.; Hubeatir, K. A.; Aadim, K. A. A novel method for zno@nio core–shell nanoparticle synthesis using pulse laser ablation in liquid and plasma jet techniques. *Scientific Reports*, **2023**, *13*, 5441. https://doi.org/10.1038/s41598-023-32330-z.